Korean Journal of Remote Sensing, Vol.38, No.1, 2022, pp.21~32
https://doi.org/10.7780/kjrs.2022.38.1.2
ISSN 1225-6161 (Print)
ISSN 2287-9307 (Online)

Article

Accuracy Comparison of TOA and TOC Reflectance Products of KOMPSAT-3, WorldView-2 and Pléiades-1A Image Sets Using RadCalNet BTCN and BSCN Data

Kwangseob Kim [1)] · **Kiwon Lee** [2)†]

Abstract: The importance of the classical theme of how the Top-of-Atmosphere (TOA) and Top-of-Canopy (TOC) reflectance of high-resolution satellite images match the actual atmospheric reflectance and surface reflectance has been emphasized. Based on the Radiometric Calibration Network (RadCalNet) BTCN and BSCN data, this study compared the accuracy of TOA and TOC reflectance products of the currently available optical satellites, including KOMPSAT-3, WorldView-2, and Pléiades-1A image sets calculated using the absolute atmospheric correction function of the Orfeo Toolbox (OTB) tool. The comparison experiment used data in 2018 and 2019, and the Landsat-8 image sets from the same period were applied together. The experiment results showed that the product of TOA and TOC reflectance obtained from the three sets of images were highly consistent with RadCalNet data. It implies that any imagery may be applied when high-resolution reflectance products are required for a certain application. Meanwhile, the processed results of the OTB tool and those by the Apparent Reflection method of another tool for WorldView-2 images were nearly identical. However, in some cases, the reflectance products of Landsat-8 images provided by USGS sometimes showed relatively low consistency than those computed by the OTB tool, with the reference of RadCalNet BTCN and BSCN data. Continuous experiments on active vegetation areas in addition to the RadCalNet sites are necessary to obtain generalized results.

Key Words: KOMPSAT-3, Pléiades-1A, RadCalNet, TOA and TOC Reflectance, WorldView-2

1. Introduction

The demand for high-resolution satellite images is growing in the fields of ecology, environmental science, and geoscience research that require an accurate analysis over the area of interest. Here, the high-resolution satellite image targets a multi-spectral image with a spatial resolution of 3 m or less and a panchromatic image of a sub-meter class. For the high-resolution images, image quality management regarding location

Received January 6, 2022; Revised January 25, 2022; Accepted February 4, 2022; Published online February 15, 2022

[1)] Part-time Lecturer, Department of Electronics and Information Engineering, Hansung University
[2)] Full Professor, Department of Electronics and Information Engineering, Hansung University

† Corresponding Author: Kiwon Lee (kilee@hansung.ac.kr)

accuracy by geometric correction or ortho-rectification, atmospheric reflectance (Top-of-Atmosphere reflectance: TOA reflectance), and surface reflectance (Top-of-Canopy reflectance: TOC reflectance) by absolute atmospheric correction is considered as an essential factor for the scientific applications, as well as radiometric calibration (https://land.copernicus.eu/global/products/toc-r).

In the case of freely distributed Landsat series and Sentinel-2 images, many experiments to verify the products of TOA and TOC reflectance have been conducted, and their results and products are released by the distribution agencies (Landsat Surface Reflectance, https://www.usgs.gov/landsat-missions/landsat-surface-reflectance Sentinel Online Level-2; https://sentinels.copernicus.eu/web/sentinel/user-guides/sentinel-2-msi/processing-levels/level-2). However, in the case of high-resolution satellite images distributed with payment, surface reflectance products are provided as value-added ones using a proprietary software by sales agencies, conducting validation experiments to evaluate accuracy (Kuester, 2017).

Typically, an atmospheric correction function calibrates the digital number (DN) values of imagery from some satellite sensors. The calibration uses sun elevation, date of acquisition, sensor gain and bias for each band to derive TOA reflectance, in addition to sun angle correction. TOC reflectance means the fraction of incoming solar radiation reflected from the Earth's surface at specific angles of incident or viewing. Atmospheric correction suppresses the scattering and absorption effects of the atmosphere to obtain the TOC reflectance characterizing the surface properties.

Some studies have been carried out in the validation of TOA and TOC reflectance products using high-resolution images and their applications. Mahiny and Turner (2007) compared atmospheric correction methods including absolute atmospheric correction and relative correction scheme such as the pseudo-invariant features (PIF) and the radiometric control sets (RCS) approaches. Manakos *et al*. (2011) compared with the field spectral data for quantitative analysis of the performance of the processed image of WorldView-2 imagery by three atmospheric correction methods, simple regression analysis, Fast Line-of-sight Atmospheric Analysis of Spectral Hypercubes (FLAASH), and Atmospheric CORrection (ATCOR). Characteristic field spectra of particular targets could provide adequate estimates of in situ reflectance using satellite data. Martin *et al*. (2012) compared the effects of Dark Object Subtraction (DOS) technique, the cosine of the sun zenith angle (COST), and Second Simulation of a Satellite Signal in the Solar Spectrum (6S) atmospheric correction methods with TOA reflectance of WorldView-2 images, and it was found that all algorithms performed the overall evaluation successfully. Especially, Radiative Transfer (RT) code of 6S model gives better results over water surfaces. Cui *et al*. (2014) investigated the performance of the Apparent Reflectance method and DOS methods for the correction of Landsat TM images. Results show that the method based on the image acquisition date and DOS iteration is superior to that based on the maximum and minimum radiances. Lee and Lee (2015) reported atmospheric correction problems with high-resolution multi-temporal images of other kinds of satellite sensors. Kim *et al*. (2015) investigated the radiometric characterization and validation of the KOMPSAT-3 sensor. Shin *et al*. (2016) suggested a calibration coefficient calculated using the TOA radiance and KOMPSAT-3 DN of the Landsat-8 overpassed at the Libya-4 site. Vuolo *et al*. (2016) compared Sentinel-2 data with atmospherically-corrected Landsat-8 data using the European Space Agency (ESA) Sen2Cor algorithm. They proposed the platform to create value-added products such as leaf area index (LAI) and broadband hemispherical-directional reflectance factor (HDRF) based on TOC reflectance as a Level-2A product. The needs and vicarious methodologies to validate the surface reflectance obtained from satellite imagery were also studied (Alonso *et al*., 2019; Badawi *et al*., 2019). Kuester (2020) has focused on the absolute radiometric calibration as a vital tool for more extensive applications of WorldView images. Pacifici (2020) expressed the importance of data quality of value-added products including reflectance products obtained from high-resolution image sets. Digital Earth Australia has expanded its national field spectroscopy campaign to validate Analysis Ready Data (ARD) for TOC reflectance products based on Landsat-8 and Sentinel-2 images (DEA Analysis Ready Data Phase 1 Validation Project, 2021).

The purpose of this study is to compare an accuracy of TOA and TOC reflectance with KOMPSAT-3 (K-3), WorldView-2 (WV-2) and Pléiades-1A (PHR-1A) images. As for the reference data as a basis for comparison, the BTCN and BSCN data in the RadCalNet portal corresponding to the date each image was acquired were used. Tools to generate the products of TOA and TOC reflectance may be critical. The Orfeo Toolbox (OTB), the only feasible tool for all three high-resolution images, was used for data processing of the three sensor images, including absolute atmospheric correction.

2. Applied Data and Processing Scheme

The high-resolution satellite specifications used in this study are given in Table 1. The three satellites were launched between 2009 and 2012, with the highest resolution from 0.46 m to 0.7 m for the panchromatic band. The spectral range is 450 nm to 1000 nm of optical satellites, and in the case of WorldView-2, the spectral range is further divided (Radiometric Use of WorldView-2 Imagery Technical Note, 2010). Compared with KOMPSAT-3, Pleiades-1A has the more similar specifications (Pléiades Imagery User Guide, 2012).

The process of comparing accuracy used in this study is depicted in Fig. 1. First, the OTB tool was used to process the generation of TOC reflectance of three types of high-resolution sensor data and Landsat-8 images. The OTB supports several operating systems with open-source satellite image software and provides optical calibration modules for TOA and TOC reflectance processing. Pléiades-1A and WorldView-2 dealt with as part of this study are mainly provided. However, KOMPSAT-3 and Landsat-8 were processed using the OTB extension modules by Lee and Kim (2019) and Kim and Lee (2021) for separate processing, not by

Table 1. Types of High-resolution satellite images used in this study

Satellite Type	Launch Date	Spectral Range	GSD (Ground Sample Distance)	Swath Width
KOMPSAT-3	May 2, 2012	450-900 nm (Panchromatic) 450-520 nm (Blue) 520-600 nm (Green) 630-690 nm (Red) 760-900 nm (NIR)	0.7 m for Panchromatic band at nadir 2.8 m for Multispectral bands at nadir	15 km (at nadir)
WorldView-2	October 8, 2009	450-800 nm (Panchromatic) 400-450 nm (Coastal Blue) 450-510 nm (Blue) 510-580 nm (Green) 585-625 nm (Yellow) 630-690 nm (Red) 705-745 nm (Red Edge) 770-895 nm (NIR1) 860-1040 nm (NIR2)	0.46 m for Panchromatic band at nadir 1.84 m for Multispectral bands at nadir	16.4 km at nadir
Pléiades-1A	December 16, 2011	480-830 nm (Panchromatic) 430-550 nm (Blue) 490-610 nm (Green) 600-720 nm (Red) 750-950 nm (NIR)	0.5 m for Panchromatic band at nadir 2.0 m for Multispectral bands at nadir	20 km at nadir

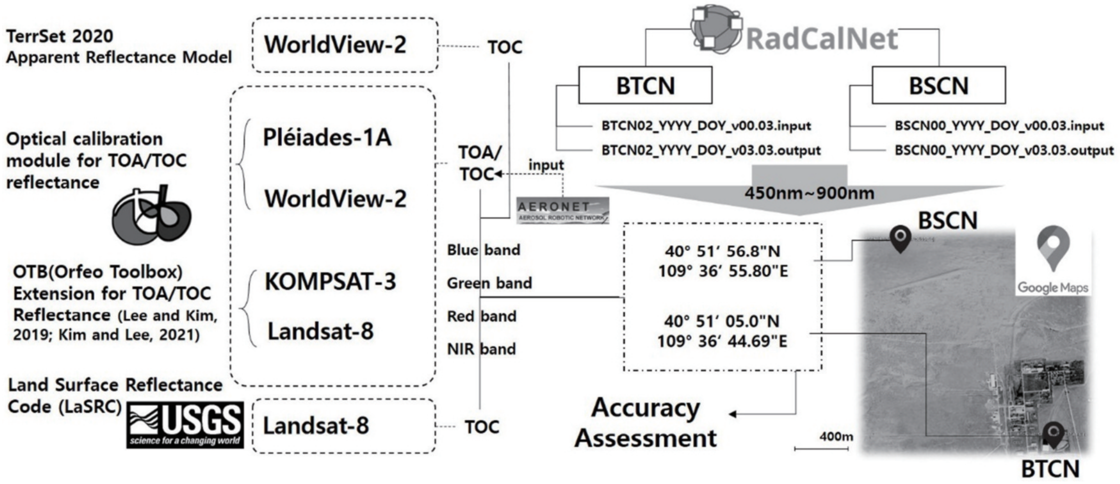

Fig. 1. Applied datasets and workflows.

default. Using the OTB extension for KOMPSAT-3A image sets, validation experiments of the TOA and TOC reflectance products based on RadCalNet data were carried out (Kim and Lee, 2020a; Kim and Lee, 2020b; Lee and Kim, 2020; Lee *et al.*, 2020).

As for Landsat-8 images, TOC reflectance products of the United States Geological Survey (USGS) obtained from the EarthExplorer site (https://earthexplorer.usgs.gov/) used it for comparative analysis with the OTB-based TOC reflectance. In contrast, the TOC reflectance products of WorldView-2 by TerrSet 2020 tool of Clark Labs were used to compare with those generated by OTB. The Apparent Reflectance function supported by TerrSet 2020 is used to adjust reflectance, or brightness, the values of some satellite imagery based on the scene illumination and sensor-gain settings (Eastman, 2016). The images are adjusted to a common illumination condition, so there should be more minor variations between scenes from different dates and sensors.

The RadCalNet portal service is managed by the Working Group on Calibration and Validation of the Committee on Earth Observation Satellites (CEOS) (Bouvet *et al.*, 2019). This free and open access portal provides SI-traceable TOA reflectance to help the radiometric calibration and validation of optical sensor data, through a network of five sites, at a 10 nm sampling interval, in the spectral range from 380 nm to 2500 nm and at 30-minute intervals, with associated uncertainties. Each site is equipped with automated ground instrumentation to provide continuous measurements of TOC reflectance and atmospheric conditions required to compute TOA reflectance values, using a common method through a central processing system. Accuracy comparisons and uncertainty analysis have been made using data from the RadCalNet BTCN and BSCN sites (Ma *et al.*, 2020) for the processed TOA and TOC reflectance products.

The data used to assess accuracy TOA and TOC reflectance are summarized in Table 2. Three high-resolution image sets, including KOMPSAT-3, Landsat-8, WorldView-2, and Pléiades-1A, were used. As for WorldView-2 and Pléiades-1A image sets, ortho-rectified data were used, and KOMPSAT-3 of Level 1G bundle image sets were used. An absolute atmospheric correction treatment by OTB was considered concerning data selection criteria. Furthermore, two conditions are needed: the reference to the comparative experiments and the atmospheric data values required for the treatment. Data from the BTCN and BSCN sites in Baotou area of China among five RadCalNet portal sites were used for reference data. The BTCN, an

Table 2. Satellite image sets used in this study: date and time of image acquisition in Universal Time Coordinated (UTC), atmospheric conditions data, and RadCalNet data. AOT means Aerosol Optical Thickness of 550 nm, and unit of the ozone amount and water vapor is Dobson and g/cm3, respectively

Date (DOY)	Satellite	Time	Atmospheric conditions			RadCalNet	
			AOT	Ozone	Water Vapor	BTCN	BSCN
07/09/2018 (190)	Landsat-8 (L-8)	03:17	0.178	0.309	1.789	BTCN02_2018_190	BSCN00_2018_190
	WorldView-2 (WV-2)	03:43					
08/15/2018 (227)	KOMPSAT-3 (K-3)	05:54	0.366	1.559	0.296	BTCN02_2018_227	–
05/09/2019 (129)	Pléiades-1A (PHR-1A)	03:17	0.291	0.345	0.615	BTCN02_2019_129	–
	WorldView-2 (WV-2)	04:40	0.340	0.346	0.603		
	Landsat-8 (L-8)	05:30	0.361	0.345	0.612		
05/15/2019 (135)	KOMPSAT-3 (K-3)	05:15	0.621	0.357	0.342	–	BSCN00_2019_133

artificial site, has been collected since April 2016 and BSCN, a naturally sandy site, since June 2017. Atmospheric values are available on the AERONET site (https://aeronet.gsfc.nasa.gov/). After verification based on image acquisition data, the data for four dates presented in Table 2 were selected. The AERONET provides three atmospheric data values required for reflectance generation processing: Aerosol Optical Thickness (AOT) of 550 nm, Ozone in Dobson unit, and water vapor in g/cm^3. The OTB supports an importing function of AERONET data for radiometric calibration processing.

The reasons that sufficient data were not used in the experiment are as follows. As for KOMPSAT-3A images, there are not many image sets for RadCalNet sites, and even if there are image sets on those sites, it is hard to find out cloud-free or less cloudy images. Moreover, in the case of RadCalNet data, the number of the day providing the actual data of the BTCN and BSCN sites in 2018 were 108 and 41, respectively (Bouvet, 2021), and there were not many cases where the KOMPSAT-3A image acquisition date and RadCalNet data existed at the same time. For 2019, data of the BTCN and BSCN sites are available only 102 and 73 days, respectively. To apply enough data for more effective findings or quantitative conclusions on this theme, new KOMPSAT-3A image sets passing through these two RadCalNet sites, as well as other three RadCalNet sites such as Gobabeb, Namibia (GONA), Railroad Valley Playa, USA (RVUS), and La Crau, France (LRCR), are necessary.

Table 3 presents the angle values for the satellites used in the study. The elevation and azimuth values of the angles of the Sun, as well as the elevation and

Table 3. Satellite image sets used in this study

Date (DOY)	Satellite	Sun Angles (in degree)		Viewing Angles (in degree)		
		Elevation	Azimuth	Elevation	Azimuth	Off-nadir
07/09/2018 (190)	Landsat-8	64.5	128.4	87.0	5.9	0.0
	WorldView-2	67.4	139.1	73.0	43.9	15.4
08/15/2018-(227)	KOMPSAT-3	61.2	206.7	74.7	261.2	13.8
05/09/2019 (129)	Pléiades-1A	63.4	147.7	83.8	6.6	6.7
	WorldView-2	65.5	160.4	59.8	302.6	27.0
	Landsat-8	61.6	138.8	87.1	5.9	0.0
05/15/2019 (135)	KOMPSAT-3	64.4	213.6	80.0	77.4	9.0

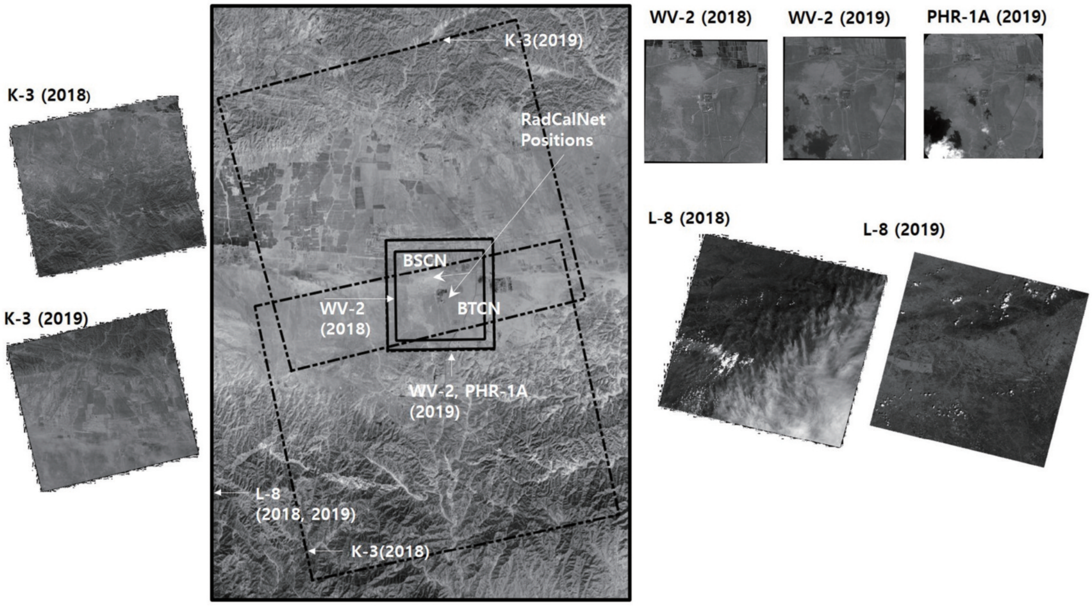

Fig. 2. Applied image sets around the RadCalNet BTCN and BSCN sites.

azimuth values of the viewing angles, are required for treatment of reflectance generation in the OTB tool.

Fig. 2 displays the image sets surrounding the RadCalNet BTCN and BTSN sites. The Landsat-8 satellite imageries cover all other data sets. Some data sets, such as Landsat-8 in 2018 and Pléiades-1A in 2019, include cloud areas, but the BTCN and BSCN sites are located outside of these areas.

3. Result and Discussion

The three types of high-resolution image data used in this study were impossible to obtain data taken simultaneously, so experiments to assess the accuracy of TOA and TOC reflectance were conducted on data obtained on as adjacent a date as possible. Therefore, the experiment results are presented on a per-sensor basis.

Fig. 3 shows TOA and the TOC reflectance products of KOMPSAT-3 by the OTB extension. Fig. 3(a) and (b) are RadCalNet-BTCN site on August 15, 2018 and RadCalNet-BSCN site on May 15, 2019, respectively. The reflectance is represented as a scale between 0.0 and 0.5, and the wavelength value ranges as blue (450-520 nm), green (520-600 nm), red (630-690 nm), and NIR (760-900 nm) from low values. For KOMPSAT-3 images, the TOA and TOC reflection results computed by the OTB extension showed more than 95% consistency with RadCalNet data. Because TOA and TOC data of the RadCalNet site at the both dates showed a fluctuation in the NIR band, uncertainty data for those data were checked out. In Figs. 3(c) and (d), it is revealed that there is no problem in data interpretation, since all data are within the range of 0.01 as uncertainty value.

Fig. 4 shows the TOA and TOC reflectance products of Landsat-8 image sets. Both BTCN and BSCN data of RadCalNet are available at the acquisition date of Landsat-8 image sets in 2018, but only BTCN data is provided at the acquisition date of Landsat-8 in 2019. Fig. 4(a) and (b) are TOA reflectance by the OTB extension at the RadCalNet-BTCN and BSCN sites on July 9, 2018 and OTB results at the RadCalNet-BTCN site on May 9, 2019, respectively. Fig. 4(c) and (d) are TOC reflectance products of OTB and USGS at the

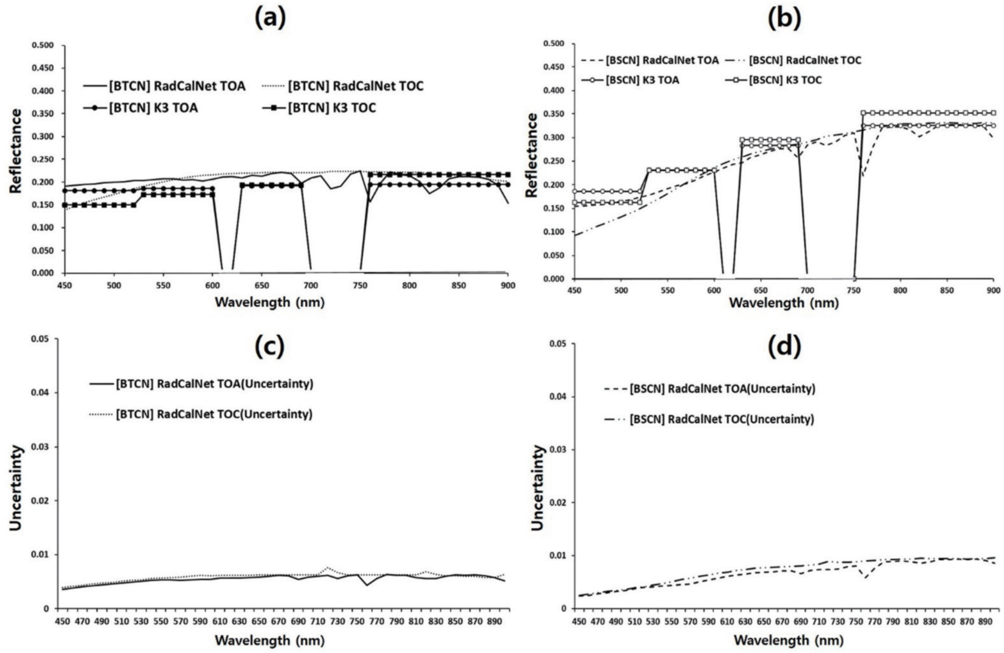

Fig. 3. Comparison results of the TOA and TOC reflectance products for KOMPSAT-3 by the OTB extension with corresponding RadCalNet uncertainty data: (a) RadCalNet-BTCN site on August 15, 2018, (b) RadCalNet-BSCN site on May 15, 2019, (c) Uncertainty of RadCalNet-BTCN site on August 15, 2018, and (d) Uncertainty of RadCalNet-BSCN site on May 15, 2019.

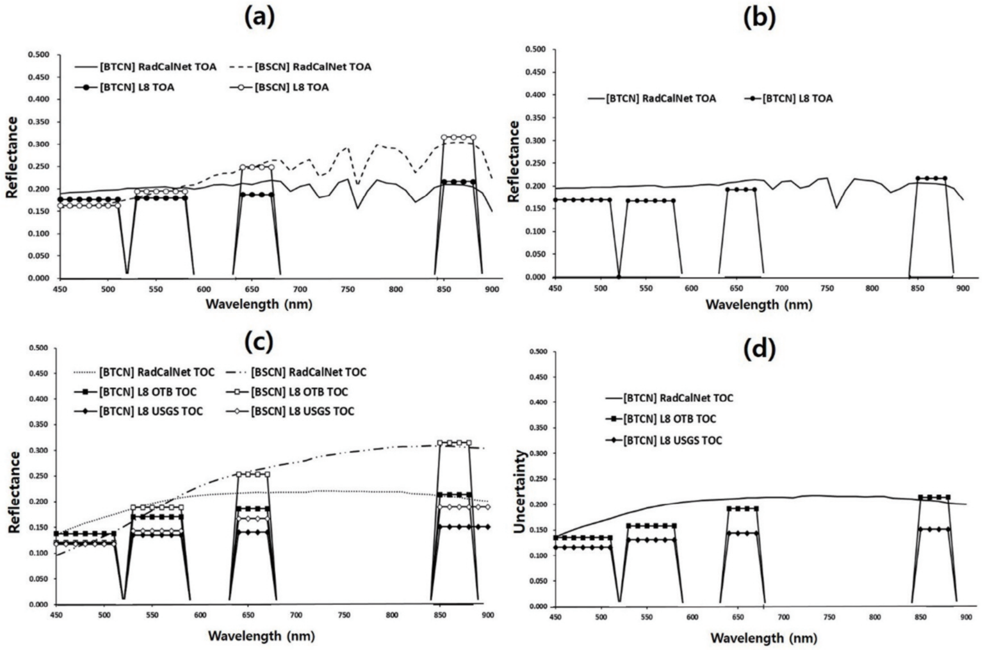

Fig. 4. Comparison results of the TOA and TOC reflectance products of Landsat-8 image sets: (a) TOA reflectance by OTB at the RadCalNet-BTCN and BSCN sites on July 9, 2018, (b) TOA reflectance by OTB at the RadCalNet-BTCN site on May 9, 2019, (c) TOC reflectance products of OTB and USGS at the RadCalNet-BTCN and BSCN sites on July 9, 2018, and (d) TOC reflectance products of OTB and USGS at RadCalNet-BTCN site on May 9, 2019.

RadCalNet-BTCN and BSCN sites on July 9, 2018 and TOC reflectance products of OTB and USGS at RadCalNet-BTCN site on 9 May, 2019, respectively. According to the results, all products of TOA reflectance in 2018 and 2019 match the corresponding RadCalNet data as shown in Fig. 4(a) and (b). The results of TOC reflectance products using the OTB extension also show a high degree of consistency with RadCalNet data, within the error limit of 5%. In addition, USGS products were found to fall outside the 5% range. It is reported that USGS Landsat-8 ARD is generated using specific algorithm named Land Surface Reflectance Code (LaSRC) (https://www.usgs.gov/landsat-missions/landsat-collection-2-us-analysis-ready-data). Ideally, no matter what method is applied, the surface reflectance calculated from the same Landsat-8 image should show the same result. Nevertheless, different results may appear depending on the algorithm or technique applied.

Although the USGS results presented here cannot be generalized as they are limited to data at a specific date, the results handled directly showed better performance if possible.

Fig. 5(a) and (b) represent TOA and TOC reflectance of WorldView-2 image sets at the RadCalNet-BTCN and BSCN site on July 9, 2018 and (b) TOA and TOC reflectance of WorldView-2 image sets at the RadCalNet-BTCN site on May 9, 2019, respectively. While, Fig. 5(c) is TOA and TOC reflectance of Pléiades-1A at the RadCalNet-BTCN site on May 9, 2019, with RadCalNet data at the same date.

The OTB created the TOA and TOC reflectance products for all images. On July 9, 2018, BTCN and BSCN data are available on the RadCalNet portal, but BSCN data on May 9, 2019 was not provided. The comparison results are highly consistent, as are those of KOMPSAT-3.

In contrast to the preceding comparison experiment,

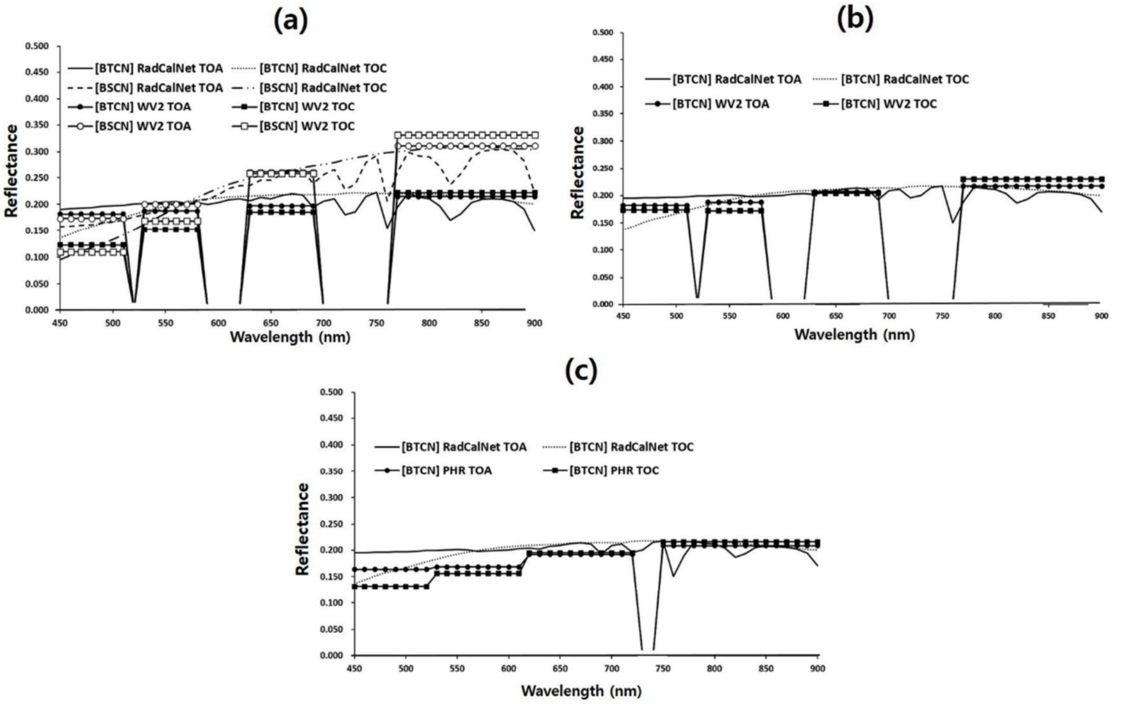

Fig. 5. (a) TOA and TOC reflectance of WorldView-2 by OTB at the RadCalNet-BTCN and BSCN site on July 9, 2018, (b) TOA and TOC reflectance of WorldView-2 by OTB at the RadCalNet-BTCN site on May 9, 2019, and (c) TOA and TOC reflectance of Pléiades-1A at the RadCalNet-BTCN site on May 9, 2019.

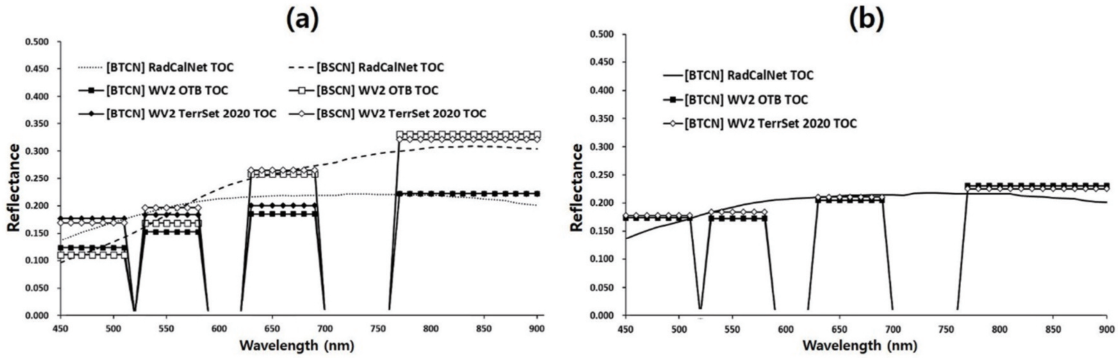

Fig. 6. (a) TOC reflectance products of WorldView-2 by OTB and TerrSet 2020 at the RadCalNet-BTCN site on July 9, 2018, and (b) TOC reflectance of WorldView-2 by OTB and TerrSet 2020 at the RadCalNet-BTCN site on May 9, 2019.

Fig. 6 shows an experiment finding to investigate the difference when different tools to generate TOC reflectance products were used. As an example using WorldView-2 image sets, TerrSet 2020 has been applied. For TOC reflectance production, TerrSet 2020 tool provides an Apparent Reflectance method, which corrects the effects caused by solar irradiance and solar zenith angle, ignoring the effects of atmospheric scattering and absorption.

Fig. 6(a) and (b) are the results using image sets on July 9, 2018 and those on May 9, 2019, respectively. As a result of the comparison, the two processes show similar flows, but the difference turned out to be very small. Unlike the absolute atmospheric correction algorithm of the OTB, which uses atmospheric environment data as an input value, the Apparent Reflection method does not require these data. Therefore, somewhat different results could be predicted, but the results of this experiment can be interpreted to show slight differences because the BSCN and BTCN sites are located in the desert area with little atmospheric effects. As a result, further studies are required in areas with active vegetation and significant atmospheric effects.

The difference between the TOA and TOC reflectance products based on OTB and data on RadCalNet sites for each band of all image sets in absolute value are summarized in Fig. 7 as bar charts for each band of blue, green, red, and NIR. Fig. 7(a) and (b) are the results of TOA reflectance products in 2018 and 2019, respectively. Fig. 7(c) and (d) present the results of TOC reflectance products in 2018 and 2019, respectively. We used the only one-pixel value for error calculation due to the homogeneous reflectance values obtained around the RadCalNet stations. Also average values within range of each band in the RadCalNet stations were applied as the reference value for each band.

In Fig. 7(a), The TOA reflectance products in 2018 showed that the NIR band in the WorldView-2 image sets had a relatively high degree of inconsistency with RadCalNet data among all products, but it falls within error range within 5%. In the case of the TOA reflectance products in 2019 as shown in Fig. 7(b), the green band of the Landsat-8 image and the blue and green bands of Pléiades-1A showed large errors compared to RadCalNet data at the same date and time, but these are also a small degree without any problems in analysis. Whereas, in the case of TOC reflectance products in 2018 as shown in Fig. 7(c), the green band of the WorldView-2 image sets shows the highest degree of inconsistency with RadCalNet data among all. Nevertheless, this poses no problem for other applications.

In the case of the TOC reflectance products in 2019 in Fig. 7(d), the green band of Pléiades-1A and the blue band of KOMPSAT-3 showed a larger degree of

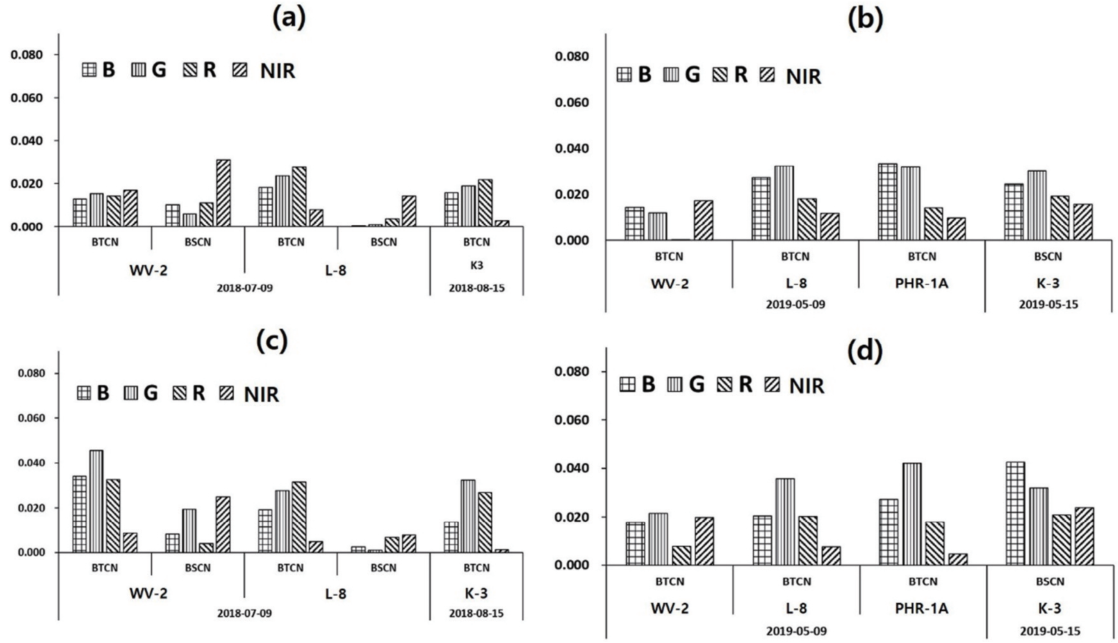

Fig. 7. The difference between TOA and TOC reflectance based on OTB and data on the RadCalNet sites for each band of all image sets in absolute value: (a) Results of TOA reflectance products in 2018, (b) Results of TOA reflectance products in 2019, (c) Results of TOC reflectance products in 2018, and (d) Results of TOC reflectance products in 2019.

inconsistency, but these are also small ones like other reflectance products. On the other hand, when comparing TOA and TOC reflectance products, TOC reflectance shows a slightly higher degree of inconsistency with RadCalNet data than TOA reflectance.

4. Concluding Remarks

The importance of the question of the extent to which the TOA and TOC reflectance of high-resolution satellite imagery corresponds to the actual surface reflectance is highlighted. Based on RadCalNet BTCN and BSCN data, this study compared the TOA and TOC reflectance accuracy of the currently available optical satellites KOMPSAT-3, WorldView-2, and Pléiades-1A image sets calculated using the absolute atmospheric correction function of the OTB tool. The comparison experiment used data from 2018 and 2019, and the Landsat-8 image sets from the same period were applied together.

The main results of this study are as follows: First, the comparison of TOA and TOC reflectance calculated from multi-spectral satellite images with spatial resolution of 3m or less using RadCalNet BTCN and BSCN measurement data as reference values showed high consistency with reference values in all cases. Second, in this study, TOA and TOC reflectance products were calculated using the OTB tool for all sensors, and the experiment results demonstrate that the tool can be applied reliably to all sensors. Third, in the case of WorldView-2 images, this result was almost consistent when comparing the results from the Apparent Reflection method, which does not use atmospheric data, with the products of TOC reflectance computed by OTB. It is interpreted that this was because the RadCalNet BTCN and BSCN sites are located in areas with little atmospheric change. Therefore, the results may differ in targeting areas where vegetation and atmospheric change are active.

Fourth, the reflectance products provided by the USGS sometimes showed more significant errors in the Landsat-8 images than the surface reflectance directly calculated by the OTB, compared with RadCalNet data. Finally, continuous experiments with active vegetation areas in addition to the RadCalNet sites are required for more accurate and wide applications.

Acknowledgements

This research was financially supported by Hansung University for Kiwon Lee. Additionally, this work was supported by the National Research Foundation of Korea (NRF) grant funded by the Korea government (MSIT) (No. 2021R1F1A1045923) for Kwangseob Kim.

References

Alonso, K., M. Bachmann, K. Burch, E. Carmona, D. Cerra, R. de los Reyes, D. Dietrich, U. Heiden, A. Hölderlin, J. Ickes, U. Knodt, D. Krutz, H. Lester, R. Müller, M. Pagnutti, P. Reinartz, R. Richter, R. Ryan, I. Sebastian, and M. Tegler, 2019. Data Products, Quality and Validation of the DLR Earth Sensing Imaging Spectrometer (DESIS), *Sensors*, 19(20): 4471.

Astrium, 2012. Pléiades Imagery User Guide, https://content.satimagingcorp.com/media/pdf/User_Guide_Pleiades.pdf, Accessed on Oct. 20, 2021.

Badawi, M., D. Helder, L. Leigh, and X. Jing, 2019. Methods for Earth-Observing Satellite Surface Reflectance Validation, *Remote Sensing*, 11(13): 1543.

Bouvet, M., K. Thome, B. Berthelot, A. Bialek, J. Czapla-Myers, N.P. Fox, P. Goryl, P. Henry, L. Ma, S. Marcq, A. Meygret, B.N. Wenny, and E.R. Woolliams, 2019. RadCalNet: A Radiometric Calibration Network for Earth Observing Imagers Operating in the Visible to Shortwave Infrared Spectral Range, *Remote Sensing*, 11(20): 2401.

Bouvet, M., 2021. Reference Calibration Validation Networks: RadCalNet, https://earth.esa.int/eogateway/documents/20142/37627/1B2_VH-RODA+2021_1B2_RadCalNet_Bouvet_v2.pdf/6a7108c3-75fa-2667-9e49-e16f42cd62c7, Accessed on Nov. 24, 2021.

Cui, L., G. Li, H. Ren, L. He, H. Liao, N, Ouyang, and Y. Zhang, 2014. Assessment of atmospheric correction methods for historical Landsat TM images in the coastal zone: A case study in Jiangsu, China, *European Journal of Remote Sensing*, 47(1): 701-716.

DEA Analysis Ready Data Phase 1 Validation Project, 2021. https://ecat.ga.gov.au/geonetwork/srv/api/records/3c018288-cb41-41c7-b099-caf6549f578f, Accessed on Oct. 20, 2021.

Eastman, J. R., 2016. TerrSet Geospatial Monitoring and Modeling System Manual, ClarkLabs, https://clarklabs.org/wp-content/uploads/2016/10/Terrset-Manual.pdf, Accessed on Nov. 20, 2021.

Kim, K. and K. Lee, 2020a. Validation of Surface Reflectance Product of KOMPSAT-3A Image Data Application of RadCalNet Baotou (BTCN) Data, *Korean Journal of Remote Sensing*, 36(6-2): 1509-1521 (in Korean with English abstract).

Kim, K. and K. Lee, 2020b. A Validation Experiment of the Reflectance Products of KOMPSAT-3A Based on RadCalNet Data and Its Applicability to Vegetation Indexing, *Remote Sensing*, 12(23): 3971.

Kim, K. and K. Lee, 2021. An Implementation of OTB Extension to Produce TOA and TOC Reflectance of LANDSAT-8 OLI Images and Its Product Verification Using RadCalNet RVUS Data, *Korean Journal of Remote Sensing*, 37(3): 449-461 (in Korean with English abstract).

Kim, J., C. Jin, C. Choi, and H. Ahn, 2015. Radiometric characterization and validation for the KOMPSAT-3 sensor, *Remote Sensing Letters*, 6(7): 529-538.

Kuester, M., 2017. Absolute Radiometric Calibration: 2016v0, https://dg-cms-uploads-production.s3.amazonaws.com/uploads/document/file/209/ABSRADCAL_FLEET_2016v0_Rel20170606.pdf, Accessed on Oct. 20, 2021.

Kuester, M., 2020. Absolute Radiometric Calibration is an Essential Tool to Imagery Science, But What is it?, https://blog.maxar.com/tech-and-tradecraft/2020/absolute-radiometric-calibration-is-an-essential-tool-to-imagery-science-but-what-is-it, Accessed on Oct. 20, 2021.

Lee, H.-S. and K.-S. Lee, 2015. Atmospheric Correction Problems with Multi-Temporal High Spatial Resolution Images from Different Satellite Sensors, *Korean Journal of Remote Sensing*, 31(4): 321-330.

Lee, K. and K. Kim, 2019. An Experiment for Surface Reflectance Image Generation of KOMPSAT 3A Image Data by Open Source Implementation, *Korean Journal of Remote Sensing*, 35(6-4): 1327-1339 (in Korean with English abstract).

Lee, K. and K. Kim, 2020. Validation of Surface Reflectance Product of KOMPSAT-3A Image Data Using RadCalNet Data, *Korean Journal of Remote Sensing*, 36(2-1): 167-178 (in Korean with English abstract).

Lee, K., K. Kim, S. Lee, and Y. Kim, 2020. Determination of the Normalized Difference Vegetation Index (NDVI) with Top-of-Canopy (TOC) Reflectance from a KOMPSAT-3A Image Using Orfeo ToolBox(OTB) Extension, *International Journal of Geo-Information*, 9(4): 257.

Ma, L., Y. Zhao, E. R. Woolliams, C. Dai, N. Wang, Y. Liu, L. Li, X. Wang, C. Gao, C. Li, and L. Tang, 2020. Uncertainty Analysis for RadCalNet Instrumented Test Sites Using the Baotou Sites BTCN and BSCN as Examples, *Remote Sensing*, 12(11): 1696.

Mahiny, A. S. and B. J. Turner, 2007. A Comparison of Four Common Atmospheric Correction Methods, *Photogrammetric Engineering and Remote Sensing*, 73(4): 361-368.

Manakos, I., K. Manevski, C. Kalaitzidis, and D. Edler, 2011. Comparison between Atmospheric Correction Modules on the Basis of Worldview-2 Imagery and In Situ Spectroradiometric Measurements, *Proc. of the 7th EARSeL SIG Imaging Spectroscopy Workshop*, Edinburgh, UK, Apr. 11-13, pp. 11-13.

Martin, J., F. Eugenio, J. Marcello, A. Medina, and J.A. Bermejo, 2012. Atmospheric correction models for high resolution WorldView-2 multispectral imagery: A case study in Canary Islands, Spain, *Proc. of SPIE, Remote Sensing of Clouds and the Atmosphere XVII; and Lidar Technologies, Techniques, and Measurements for Atmospheric Remote Sensing VIII,* Edinburgh, UK, Sep. 24-27, vol. 8534, p. 85340O.

Pacifici, F., 2020. Future of Remote Sensing and Data Quality, https://calval.cr.usgs.gov/apps/sites/default/files/jacie/2020-S5-Pacifici-Future_Remote_Sensing_Data_Quality.pdf, Accessed on Oct. 20, 2021.

Radiometric Use of WorldView-2 Imagery Technical Note, 2010. https://dg-cms-uploads-production.s3.amazonaws.com/uploads/document/file/104/Radiometric_Use_of_WorldView-2_Imagery.pdf, Accessed on Oct. 20, 2021.

Shin, D.Y., H.Y. Ahn, S.G. Lee, C.U. Choi, and J.S. Kim, 2016. Radiometric Cross-calibration of KOMPSAT-3A with Landsat-8, *International Archives of the Photogrammetry, Remote Sensing and Spatial Information Sciences*, 41(B1): 379-382.

Vuolo, F., M. Zoltak, C. Pipitone, L. Zappa, H. Wenng, M. Immitzer, M. Weiss, F. Baret, and C. Atzberger, 2016. Data Service Platform for Sentinel-2 Surface Reflectance and Value-Added Products: System Use and Examples, *Remote Sensing*, 8(11): 938.